Seismic triggering in a stable continental area: The Lugo 1995–1997 seismic sequences (NW Spain)

J.J. Martínez-Díaz [a,*], R. Capote [a], M. Tsige [a], P. Villamor [b], F. Martín-González [c], J.M. Insua-Arévalo [a]

[a] *Dpto. de Geodinámica, Facultad de Ciencias Geológicas, Universidad Complutense c/José Antonio Novais s/n, 28040 Madrid, Spain*
[b] *Institute of Geological and Nuclear Sciences, Gracefield Research Center, 69 Gracefield Road, Gracefield, P.O. Box 30368, Lower Hutt, New Zealand*
[c] *Escuela Superior de CC, Experimentales y Tecnología, Universidad Rey Juan Carlos, C/Tulipán s/n 28933 Móstoles, Madrid, Spain*

Abstract

The northwestern area of the Iberian Peninsula traditionally is considered a seismically stable area. However, since 1979 this region has experienced a significant increase in seismic activity. In 1995 and 1997, two earthquakes, with magnitude M_w 4.2 and 5.1, respectively, caused significant damage in the region (intensity EMS: V). In this work, we analysed the focal mechanisms that had the most coherence with the local structures and tectonics. Modelling of the coseismic Coulomb static stress changes generated by the 1995 sequence was performed in order to find a possible genetic relationship with the 1997 sequence. Models using oblique (reverse strike-slip) movement on a fault with the same geometry and orientation as the Baralla fault, mapped at the surface, yield the best fit with the spatial distribution of the 1997 sequence. The existence of causal relationships between two close seismic sequences is important for the improvement of future seismic hazard assessments methodologies.

Keywords: Seismic sequence; Galicia; Focal mechanisms; Seismotectonics; Coulomb stress change; triggering

1. Introduction

In recent years, several seismic series have occurred in continental areas that are classified as stable. Up to 11 earthquakes that produced surface rupture in stable continental areas of Australia, North America and Africa from 1819 to 2001 have been documented (Crone et al., 1992; Crone and Machette, 2001). Most of these earthquakes indicated that faults considered seismically inactive during the historical period are capable of generating $M > 6$ earthquakes. The damages produced by these unexpected earthquakes are usually stronger than the damages produced by similar earthquakes in more active areas because of poor building practices.

The short period of time covered by the modern high quality seismic network (from 1980, I.G.N., 1991), the scarcity of the historical record, and the large recurrence interval typical of faults in stable continental areas with low

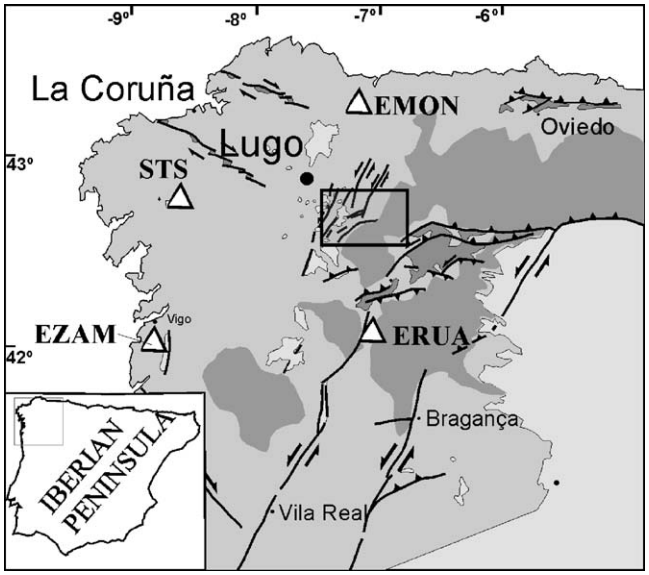

Fig. 1. Tectonic setting of the northwestern area of the Iberian Peninsula. The white triangles are the seismic stations of the regional Spanish Seismic Network.

deformation rates like the NW of the Iberian Peninsula may lead to unexpected shocks like the sequences analysed in this work.

The first instrumental record of seismic activity in the surrounding area of the Sarria basin took place in 1979, with two earthquakes of magnitudes M_w 4.2 and 4.4 located 20 km to the north of Becerreá (Rueda and Mezcua, 2001), probably associated with other sources seismic, different from the faults studied in this work. After a period of quiescence, the seismic activity restarted in the Lugo region in 1995 with two earthquakes of magnitude M_w 4.2 (November 29 and December 24) and their aftershock series. A second sequence occurred in May 1997 with a M_w 5.1 main shock. These two sequences revealed a rather high seismic activity rate. The region is part of the Iberian massif, which has been considered relatively stable with a low seismicity level. Before 1979, neither historical nor instrumental seismicity was known in the study area. Local geology shows the presence of an alpine structure related to the uplift of the Cantabrian-Leoneses Ranges during the Tertiary. This structure is controlled by faults possibly reactivated by the recent seismicity (Capote et al., 1999) (Fig. 1).

The identification of seismogenic sources in this area, considered up to now a stable continental region, justifies a geologic and seismotectonic analysis of the seismic sequences in Lugo.

The focal mechanisms determined in previous works for these series give variable solutions that differ on the authors and on the method of inversion: the centroid moment tensor method (Dziewonsky and Woodhouse, 1983; Harvard CMT Catalogue) or the first arrival polarities method. The first method supports normal faulting mechanisms and the second method indicates reverse faulting (Rueda and Mezcua, 2001, 2005) and normal faulting (Herráiz et al., 2000) (Figs. 2 and 3). In this work, we present a seismotectonic interpretation of the Lugo sequences using geological and seismological data. We have performed several models of Coulomb static stress changes induced by the 1995 earthquake in order to determine if there is a genetic relationship (triggering effect) with the 1997 seismic sequence.

2. Tectonic setting

The alpine structure of the zone is characterised by a NE–SW reverse fault zone that contributes to the uplift of the region located to the southeast of the study area, the Cantabrian-Leoneses Ranges (Fig. 1). This mountainous area has been interpreted as the rear limb of a fault-bend fold, which formed over a basement unit thrusting the Duero and El Bierzo basins (Santanach, 1994). The faults that form the reverse fault zone affect the basement and control the geometry of Miocene sedimentary basins. The Sarria basin is the larger basin and its northwestern border is controlled

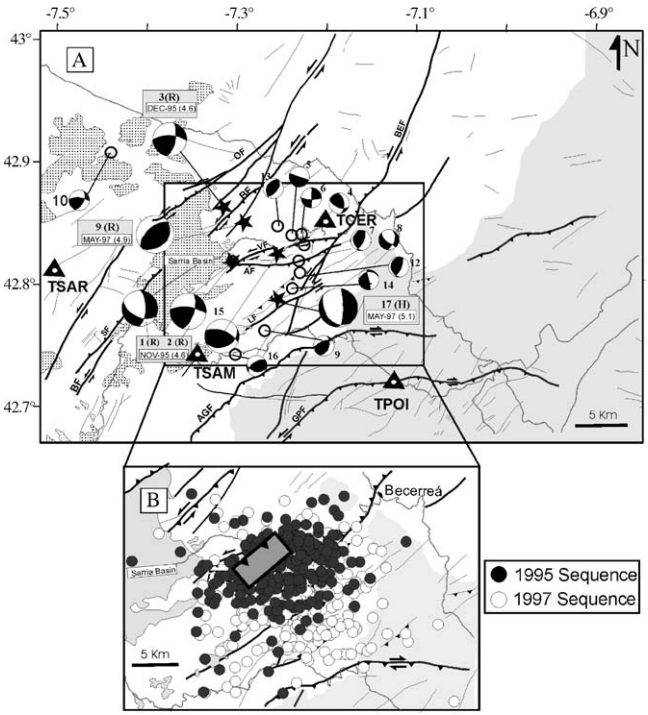

Fig. 2. (A) Tectonic map of the study area (see the situation in Fig. 1). OF: Outeiro fault; BF: Baralla fault; VF: Villaesteve fault; BEF: Becerreá fault; AF: Armada fault; LF; Loureiro fault; AGF: Agradelo fault; GPF: Gundaiz-Piedrafita fault. The focal mechanisms of the main shocks and aftershocks of the 1995 and 1997 series are shown. The focal mechanisms are labelled R for those calculated by Rueda and Mezcua (2001) and Mezcua (2000), S for those calculated by Herráiz et al. (2000) using first arrival polarities and H for Harvard CMT catalogue data. Focal mechanisms of the same event calculated with different methods or from different authors are included in a white rectangle. See Fig. 3 to observe the polarity data. White areas on the map represent the hercinian basement, the dotted area represents the Miocene sedimentary basins. The grey area represents the hercinian mountains more than 1000 m high. The black triangles shows the position of the portable digital seismic stations installed around the seismic area. (B) Map view of the aftershocks of the 1995 and 1997 series projected on the map of fractures. The grey rectangle shows the map view projection of the rupture area of the Baralla fault modelled in the stress change calculation program.

by fault activity. From structural mapping of the area two families of faults showing alpine tectonic activity are observed:

- *Reverse ENE-WSW faults: Agradelo and Gundaiz-Piedrafita faults* (Fig. 2). These faults have a curved and anastomosing geometry, with slip surfaces dipping 45–50° to the southeast. In the central part of the fault traces, movement indicates a pure reverse movement whereas toward the two tips they show a strike-slip component with dextral movement at the eastern tip and sinistral movement at the western tip (Fig. 2). To the northwest of Triacastela village, minor thrust faults occur (Armada and Villaesteve faults). The traces of all these faults and the spatial distribution of the strike-slip tips are coherent with a NW–SE shortening direction.
- *Sinistral NNE–SSW faults*. These structures are steeply-dipping reverse faults. Some of them dip to the northwest (Becerreá, Outeiro and Sarria faults; Fig. 2) and one to the southeast (Baralla fault). The traces of these faults are more linear. However, they occasionally present some inflections that behave as restraining bends (near Becerreá) or releasing bends, with corresponding push-up and small pull-apart structures.

3. The 1995–1997 seismic sequences

The seismic data utilised in this study was detected and located by the National Seismic Network managed by the Instituto Geográfico Nacional (www.geo.ign.es). The main shock and the aftershocks were surrounded by four stations of this regional network (STS, EZAM, EMON and ERUA in the Fig. 1). To increase the completeness of the coverage, a local network with four digital portable seismographs (TSAR, TSAM, TPOI and TCER in the Fig. 1) was installed

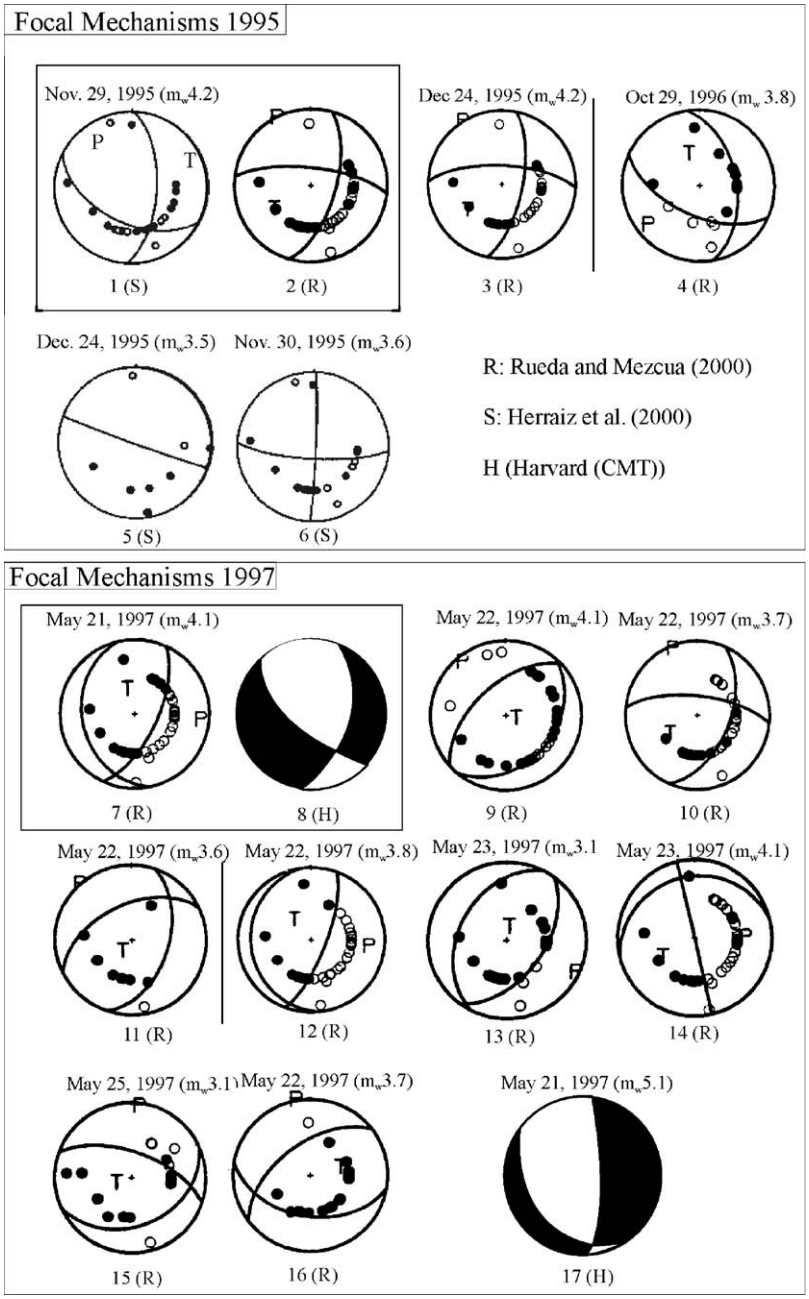

Fig. 3. Focal mechanisms of the main events during the seismic sequences of 1995 and 1997. Focal mechanisms of the same event calculated with different methods or from different authors are included in a white rectangle. Polarity data are shown in first arrival polarities solutions.

after the occurrence of the 1995 main shock. These local seismic stations circled the active zone. They monitored the seismic activity during several months and guaranteed the detection of all the $M_w > 3$ earthquakes.

The first significant seismic activity recorded in the area started in 1995. This activity consisted of two small sequences (Table 1). Parameters of the aftershocks with RMS < 0.3 s are shown in Table 2 (data from the Instituto Geográfico Nacional of Spain; www.geo.ign.es). The first sequence started with a M_w 4.2 event on November 29 followed by 32 $M_w > 2.5$ aftershocks in 24 h. The aftershock rate decayed over the next 20 days (Fig. 4). The second sequence started with a M_w 4.2 earthquake on December 24. The rate of aftershock activity following this event was

Table 1
Parameters of the main shocks occurred in the two studied series

Longitude (UTM 29)	Latitude (UTM 29)	Magnitude (M_w)	Intensity (EMS)	Date (y/m/d)	Time	Depth (km)	ERH (km)	ERZ (km)	RMS
−7.303	42.816	4.2	V–VI	1995/11/29	23:56:28	9	1	2	0.7
−7.315	42.859	4.2	V–VI	1995/12/24	14:29:21	15	2	3	0.7
−7.258	42.783	5.1	VI	1997/5/21	23:50:45	13	2	2	0.7
−7.293	42.848	4.1		1997/5/22	00:17:19	17	2	2	0.8

Data from the Instituto Geográfico Nacional of Spain. ERH, ERZ: horizontal and vertical error of location. RMS in seconds.

lower. Most of aftershocks were located to the east of the Sarria tertiary basin (Fig. 2). The epicentres form a cluster in map view (Fig. 1). During 1996 and 1997, all aftershock had magnitudes lower than M_w 4.1.

On May 21, 1997 the second seismic series started with a M_w 5.1 event (Fig. 4). The main shock was preceded by a M_w 4.1 foreshock by 59 s. The aftershock sequence was very intense, with 106 $M_w > 2.0$ events in the 24 h following the main shock. The three main shocks of the two series reached a maximum intensity of EMS V and VI.

Table 2
Parameters of the aftershocks with RMS < 0.3 s

Longitude (UTM 29)	Latitude (UTM 29)	Magnitude (m_b)	Date (y/m/d)	Time	Depth (km)	ERH (km)	ERZ (km)	RMS (s)
−7.228	42.776	3.3	1995/11/30	0:23:30	9	1	1	0.1
−7.278	42.804	3	1995/12/11	7:54:18	5	1	2	0.2
−7.210	42.809	3	1995/12/18	4:4:55	15	2	2	0.2
−7.212	42.834	3	1995/12/24	16:15:45	13	1	2	0.2
−7.245	42.804	3.1	1995/12/24	14:48:59	11	1	1	0.2
−7.238	42.808	3	1996/2/19	12:46:13	8	2	3	0.2
−7.268	42.801	3	1996/2/19	12:43:50	4	1	2	0.1
−7.220	42.826	3	1996/8/11	11:15:35	3	1	2	0.1
−7.223	42.798	3.2	1997/2/4	13:51:11	8	2	3	0.2
−7.173	42.763	3	1997/5/22	7:9:32	11	1	1	0.2
−7.237	42.779	3	1997/5/22	4:49:1	16	1	2	0.2
−7.183	42.798	3.1	1997/5/22	1:29:9	16	2	3	0.2
−7.247	42.804	3.2	1997/5/22	0:10:6	16	2	2	0.2
−7.230	42.779	3.5	1997/5/22	16:16:43	14	1	1	0.2
−7.202	42.781	3.6	1997/5/22	0:42:34	9	2	2	0.2
−7.200	42.824	3	1997/5/22	3:51:54	7	5	1	0.1
−7.237	42.814	3.2	1997/5/22	10:57:23	14	1	1	0.1
−7.225	42.783	3	1997/5/24	19:44:47	9	1	1	0.1
−7.222	42.788	3	1997/5/24	23:20:32	11	0	0	0.0
−7.235	42.796	3	1997/5/25	8:11:41	12	1	1	0.2
−7.238	42.793	3.4	1997/5/27	23:15:22	9	1	2	0.2
−7.183	42.789	3.2	1997/5/28	20:3:48	9	1	2	0.2
−7.248	42.781	3.3	1997/5/28	2:44:57	11	1	1	0.1
−7.305	42.709	3	1997/5/31	4:21:31	18	3	1	0.2
−7.282	42.746	3.2	1997/6/3	0:12:28	14	2	1	0.2
−7.210	42.776	3.3	1997/6/5	9:59:17	9	1	2	0.2
−7.228	42.803	3.3	1997/6/5	9:7:53	9	2	2	0.2
−7.198	42.761	3.3	1997/6/5	9:58:45	11	1	1	0.1
−7.342	42.836	3.2	1997/6/28	4:53:8	15	1	2	0.1
−7.208	42.763	3	1997/8/5	13:54:22	9	1	1	0.1
−7.205	42.758	3	1997/8/5	19:28:0	11	1	1	0.1
−7.222	42.799	3.6	1997/8/7	5:54:23	13	1	2	0.2
−7.217	42.786	3.1	1997/8/7	5:54:48	10	1	1	0.1
−7.225	42.786	3.1	1997/8/7	5:52:37	10	1	1	0.1
−7.228	42.793	3.1	1997/8/11	17:12:16	16	2	2	0.2
−7.225	42.788	3.2	1997/8/11	23:11:11	12	1	1	0.1
−7.268	42.783	3	1997/10/21	16:21:40	9	1	2	0.1

Data from the Instituto Geográfico Nacional of Spain (www.geo.ign.es). ERH, ERZ: horizontal and vertical error of location.

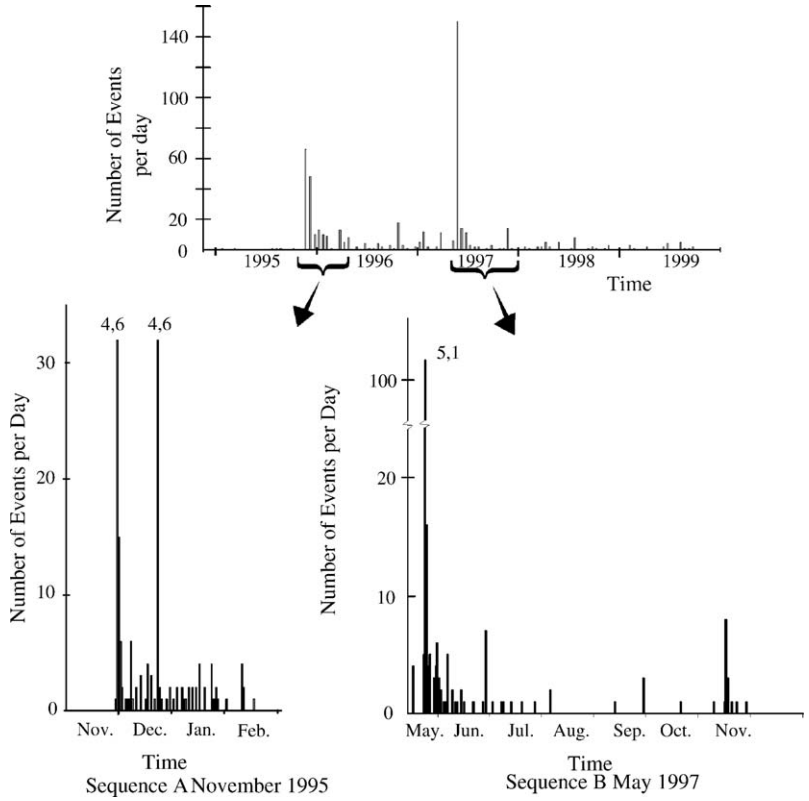

Fig. 4. Temporal evolution of the number of events in the study area from the beginning of the 1995 seismic series.

4. Tectonic structures associated to the 1995 and 1997 sequence

The distribution of aftershocks helps to identify the tectonic structures that were reactivated by the main shocks. Only the accurately located events (RMS < 0.3 s and vertical error < 3 km) were used in our following interpretation. The main events of both series are located on the eastern border of the Sarria tertiary basin (Fig. 2). The projection in map view and in cross-section of the aftershocks, shows a spatial distribution of hypocentres similar to the complete aftershock cluster (A and B in Fig. 5). The NNE–SSW cross-section of aftershocks distribution for both earthquakes shows a planar geometry dipping 65° towards the SE (B1 in Fig. 5). Analysis of the spatial distribution of aftershocks separately (C1 and C2 in Fig. 5), suggests that most of the 1995 events were located at depths between 2 and 9 km, while most of the 1997 aftershocks were located at depths between 7 and 15 km.

In the cross-section B1 of Fig. 5 we observe that the main shock of the 1995 sequence was located in the western border of the aftershock cluster, while the main shock of the 1997 sequence was located more than 5 km to the west.

The upward extension of the longer axis of the aftershock distribution coincides with the position of the Baralla fault trace (Fig. 5). The geological map shows that this fault has a more than 20 km long fault trace with a fault plane dipping 65° towards the east. Regional seismic lines support that the crust in this area is 31 km thick (Cordoba et al., 1987). The usual width-to-length ratio of faults (Wells and Coppersmith, 1994) indicate that a 20-km long fault can reach is more than 15 km in depth.

We assume that the Baralla fault has a planar geometry. This fault has a trend oblique to the geological formations of granite and metamorphic rocks, and there are no structural data from the geologic maps that support the possibility of a listric geometry for the steeply-dipping NE–SW faults in the study area. The coincidence in the position of the aftershocks for the two (1995 and 1997) seismic series suggests that both were produced by the reactivation of the Baralla fault or by a nearby source like the Becerreá fault. The position of aftershocks of the 1997 sequence shows an alignment with the Becerreá fault trace (B1 in Fig. 5). The larger depth of the hypocentres for the 1997 seismic sequence

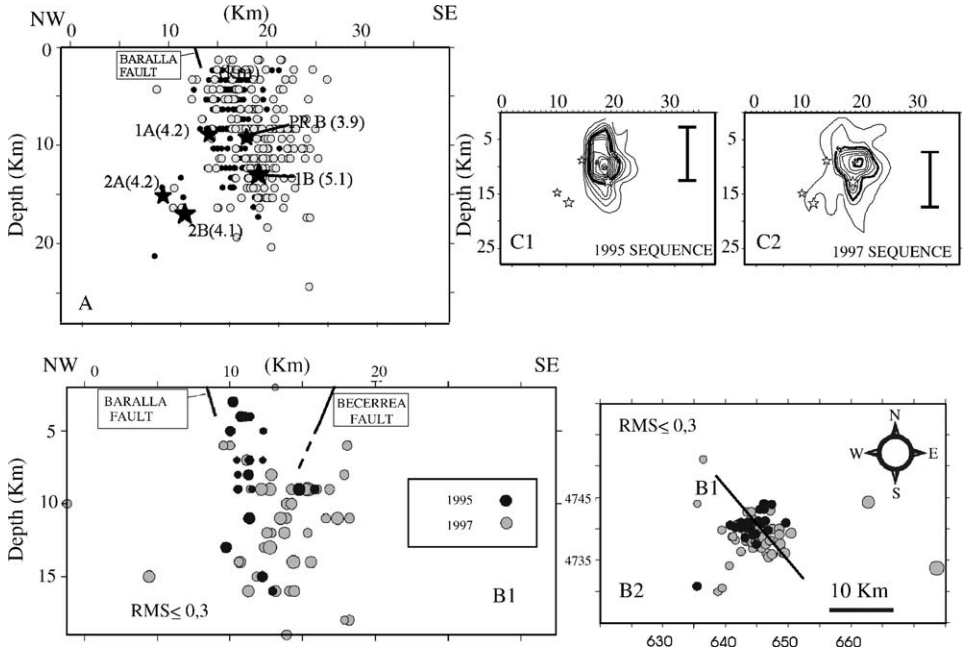

Fig. 5. (A) NW–SE oriented cross-section of the hypocentres of the main shocks and aftershocks of the 1995 (black points) and 1997 (grey points) seismic series. This section is perpendicular to the strike of the Baralla fault. (B1 and 2) cross-section and map view of the well located aftershocks of both series with RMS < 0.3 s. (C) NW–SE cross-section of the hypocentral density of the 1995 and 1997 series of aftershocks. The lines represent equal number of aftershocks and show us that the 1997 is slightly deeper than the 1995 sequence.

could indicate the propagation of the activity of the fault in the dip direction of the Baralla fault. This interpretation agrees with the focal mechanisms of Rueda and Mezcua (2001).

5. Stress transfer modelling

Our modelling of Coulomb stress changes generated by the first main shocks is two-fold: to determine the existence of a possible genetic relationship between the two seismic series, and to explain the geometry and kinematics of the source of both earthquakes. According to the fracture criteria of Coulomb, a fault plane is activated when the Coulomb stress on the plane exceeds a value specified by:

$$\mathrm{CFS} = \tau_\beta - \mu(\sigma_\beta - p)$$

where τ_β is the shear stress on the fault plane, σ_β the normal stress, P the fluid pressure and μ is the friction coefficient. Recent studies suggest that seismic-generated Coulomb Stress changes of less than 0.5 bars are able to trigger the reactivation of proximal faults close to their strength threshold (as an aftershock or as a main earthquake) (King et al., 1994; Harris et al., 1995). In this case, small magnitude earthquakes, such is the 1995 main shock, could potentially trigger other earthquakes in the area.

In the present study, the static Coulomb stress change (ΔCFS) was estimated with the equation $\Delta\mathrm{CFS} = \Delta\tau_\beta - \mu'(\Delta\sigma_\beta - \Delta p)$), where $\Delta\tau_\beta$ is the change in shear stress on a receiver fault, $\Delta\sigma_\beta$ the change in normal stress acting on the receiver fault and μ' is the apparent coefficient of friction which includes the effects of pore fluid and the material properties of the fault zone (see Harris, 1998). $\Delta\tau_\beta$ is considered positive in the direction of the fault slip. Positive values of ΔCFS promote fault rupture, while negative values inhibit activity. The stress change has been calculated in an elastic half-space using the Okada (1992) equations included in the software GNSTRESS 5.1, developed by R. Robinson from the GNSI of New Zealand. Calculations were done using a shear modulus of $33.2 \times 10^{10}\ \mathrm{N\,m^{-2}}$ a Poisson ratio of 0.25 and an apparent friction coefficient of 0.4 that is an acceptable value according to Deng and Sykes (1997). In any case, the introduction of different values for the apparent fric-

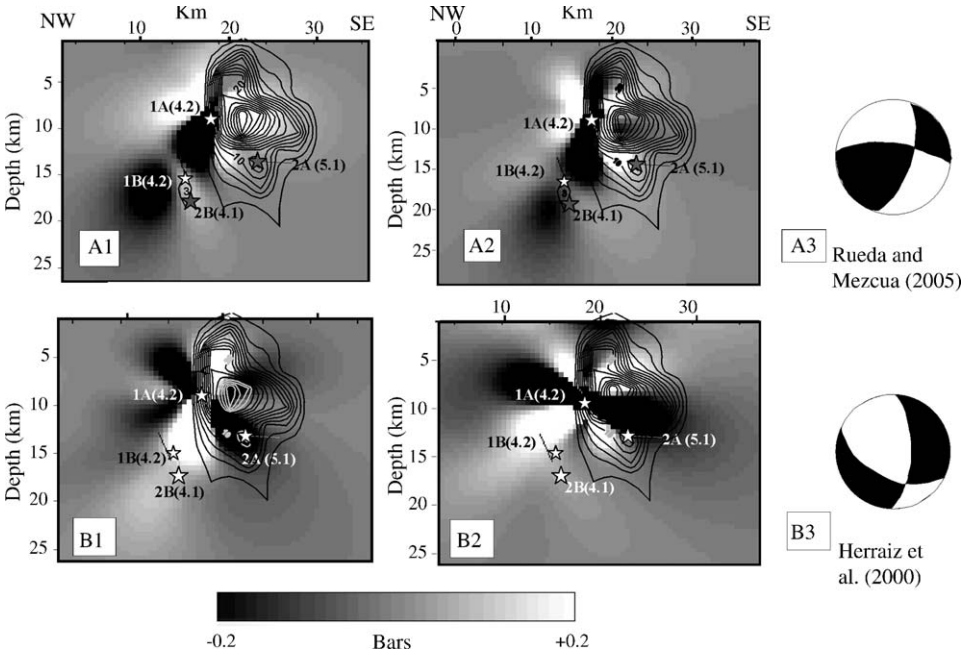

Fig. 6. Models of the static Coulomb stress transfer generated by the two main shocks of magnitude 4.6 of the 1995 sequence on planes parallel to a reverse strike-slip Baralla fault (A1) (plane NNE–SSW in the focal mechanisms of Rueda and Mezcua, 2001). (A2) Changes on planes ideally oriented with the regional stress field. In the lower part, two models constructed considering a normal kinematics for two driving faults with a similar orientation (Baralla fault) (plane NNE–SSW in the focal mechanism of Herráiz et al., 2000). (B1) Changes on planes parallel to a normal slip Baralla fault. (B2) Changes on planes ideally oriented with the regional stress field. We projected on the models the lines of hypocentral density (see Fig. 5) and the hipocentres of the aftershocks and the main events of 1995 and 1997 series. See explanation in the text.

tional coefficient did not produce significant changes in the results. For a detailed discussion of the method see Harris (1998).

Two static stress change models using the geometry of two different faults were constructed. In the first model we assumed that the 1995 main shock occurred on the Baralla fault, a reverse strike-slip fault with a plane N 35° dipping 65° towards the east. This model is consistent with one of the plane solutions of the focal mechanisms calculated by Rueda and Mezcua (2001, 2005) for (M_w 4.2) events.

The second model assumes the geometry of a normal fault with a plane NNE dipping 60° towards the east. This orientation is derived from the focal mechanism calculated by Herráiz et al. (2000). The area of surface rupture was determined using the empiric relationships of Wells and Coppersmith (1994). Both models utilised a 15 km^2 rectangular rupture with a coseismic slip of 0.08 m.

For each model two CFS calculations were made. The Coulomb stress change was calculated on planes parallel to the assumed 1995 fault rupture, and on planes which are ideally oriented to failure within the regional stress field (maximum horizontal stress NW–SE from Herráiz et al. (2000)). The results are shown on Fig. 6.

The results in Fig. 6 show the CFS changes projected in cross-section for the two reverse faulting models. Both models indicate that the main shocks of the 1997 sequence occurred in segments of the reverse Baralla fault zone where the change in CFS goes beyond 0.1 bar. The majority of the aftershocks for both series (1995 and 1997) occurred in the zone of CFS increase. Shallow aftershocks with $M_w > 3.0$ following the 1997 event occurred in lobes of CFS increase situated on the Baralla fault.

6. Discussion

The two calculations of Coulomb stress change using a reverse strike-slip fault model suggest that the first seismic event, M_w 4.2 (1995), could have occurred on a reverse fault plane oriented parallel to the Baralla fault. This event induced a positive Coulomb failure stress change of more than 0.2 bars (white areas in Fig. 6) reaching in

some areas up to 1.5 bars. Most of the aftershocks of the 1995 series as well as the main shock and the aftershocks of the 1997 sequence were located inside this area of stress increase. Moreover, the (M_w 4.1) aftershock of the 1997 series was also situated in an area of a slight increase of CFS. Therefore, there is a good correlation between the area of increase produced by the 1995 main shock that ruptured along a reverse strike-slip fault (the Baralla fault) and the position of the 1997 seismic series position. The models using normal fault kinematics do not show such a correlation. In these models most of the aftershocks and main shocks occurs in areas of stress decrease.

7. Conclusion

We conclude that, among all the models developed using the geometry of the faults mapped in the area, the fault that best explains the spatial distribution of 1997 seismic series is a southeast, steeply (65°) dipping N 30°E fault plane parallel to the Baralla reverse fault. As mentioned above, this plane also coincides with one of the nodal planes of the focal solution given by Rueda and Mezcua (2001).

The depth of the second (1997) seismic series may indicate that the first (1995) series (generated by the rupture of the Barralla fault) induced a significant CFS change on a deeper segment of the fault, loaded with a positive Coulomb failure stress change. This segment ruptured one year later and led to the 1997 seismic sequence. Another possibility is the reactivation of the deepest segment of the Becerreá fault.

The evolution of the two seismic series supports the existence of a triggering process generated by the static Coulomb stress CFS change induced by the first (M_w 4.2) event. The existence of genetic relationships between two close seismic events has great importance in future seismic hazard assessments. It has been demonstrated that changes in Coulomb static stresses produce changes in seismic probability. A sudden stress change will alter the time until the next large earthquake by the ratio of the stress change on the fault to its long-term stressing rate (Stein, 1999).

Acknowledgements

We thank Russell Robinson for his assistance and permission to use the GNSTRESS 5.1 software to calculate Coulomb stress changes. We thank to the anonymous reviewers and also thank to G. Renalli, for their careful revisions of the manuscript and for their contributions to improve this work.

References

Capote, R., Martínez-Díaz, J.J., Villamor, P., Tsige M., 1999. El marco tectónico de la sismicidad en el área de Sarria-Triacastela-Becerrea (provincia de Lugo). I Asamblea Hispano Portuguesa de Geodesia y Geofisica, IX Asamblea Nacional de Geodesia y Geofísica. Extended abstracts, Almería, Spain (CD-ROM; ISBN 84-95172-10-0).

Cordoba, D., Banda, E., Ansorge, J., 1987. The Hercynian crust in northwestern Spain: a seismic survey. Tectonophysics 132, 321–333.

Crone, A., Machette, M.N., Bowman, R., 1992. Geologic investigations of the 1988 Tennant creek, Australia, earthquakes—implications for paleoseismicity in stable continental regions. U.S. Geol. Survey Bull. 3032, 1–51.

Crone, A., Machette, M.N., 2001. Earthquakes and fault behaviour in stable continental regions—seismic hazards in unexpected places. In: Capote, R., Martínez-Díaz, J.J. (Eds.), El Riesgo Sísmico. Prevención y Seguro. Consorcio de Compensación de Seguros Publication, Madrid, pp. 93–103.

Deng, J., Sykes, L.R., 1997. Stress evolution in southern California and triggering of moderate-, small-, and micro-sized earthquakes. J. Geophys. Res. 102, 411–435.

Dziewonsky, A.M., Woodhouse, J.H., 1983. An experiment in the systematic study of global seismicity: centroid moment tensor solutions for 201 moderate and large earthquakes of 1981. J. Geophys. Res. 88, 3247–3271.

Harris, R.A., Simpson, R.W., Reasenberg, P.A., 1995. Influence of static stress changes on earthquake locations in southern California. Nature 375, 221–224.

Harris, R.A., 1998. Introduction to special session: stress triggers, stress shadows, and implications for seismic hazard. J. Geophys. Res. 103, 24347–24358.

Herráiz, M., De Vicente, G., Lindo-Ñaupari, R., Giner, J.L., Somón, J.L., González-Casado, J.M., Vadillo, O., Rodríguez-Pascua, M.A., Cicuéndez, J.I., Casas, A., Cabañas, L., Rincón, P., Cortés, A.L., Ramírez, M., Lucini, M., 2000. The recent (upper Miocene to Quaternary) and present tectonic stress distributions in the Iberian Peninsula. Tectonics 19-4, 762–786.

I.G.N., 1991. Spanish National Seismic Network. In: Mezcua, Udías (Eds.), Seismicity, Seismotectonics and Seismic Risk of the Ibero-Maghrebian Region, Serie Monografías, vol. 8. I.G.N., Madrid, pp. 3–15.

King, G.C.P., Stein, R.S., Lin, J., 1994. Static stress changes and the triggering of earthquakes. Bull. Seismol. Soc. Am. 84, 935–953.

Okada, Y., 1992. Internal deformation due to shear and tensile faults in a half space. Bull. Seismol. Soc. Am. 82, 1018–1040.

Rueda, J., Mezcua, J., 2001. Sismicidad, Sismotectónica y Peligrosidad Sísmica en Galicia, vol. 35. IGN Publication, Madrid, 64 pp.
Rueda, J., Mezcua, J., 2005. Near-real-time moment-tensor determination in Spain. Seismol. Res. Lett. 76-4, 456–465.
Santanach Prat, P., 1994. Las cuencas terciarias gallegas en la terminación occidental de los relieves pirenaicos. Cuadernos Laboratorio Xeolóxico de Laxe 19, 57–71.
Stein, R.S., 1999. The role of stress transfer in earthquake recurrence. Nature 402, 605–609.
Wells, D.L., Coppersmith, K., 1994. New empirical relationships among magnitude, rupture length, rupture width, rupture area and surface displacement. Bull. Seismol. Soc. Am. 84, 974–1002.